Science in China Series G: Physics, Mechanics & Astronomy

Rapid solidification and dendrite growth of ternary Fe-Sn-Ge and Cu-Pb-Ge monotectic alloys

ZHANG XueHua, RUAN Ying, WANG WeiLi & WEI BingBo†

Department of Applied Physics, Northwestern Polytechnical University, Xi'an 710072, China

The phase separation and dendrite growth characteristics of ternary Fe-43.9%Sn-10%Ge and Cu-35.5%Pb-5%Ge monotectic alloys were studied systematically by the glass fluxing method under substantial undercooling conditions. The maximum undercoolings obtained in this work are 245 and 257 K, respectively, for these two alloys. All of the solidified samples exhibit serious macrosegregation, indicating that the homogenous alloy melt is separated into two liquid phases prior to rapid solidification. The solidification structures consist of four phases including α-Fe, (Sn), FeSn and $FeSn_2$ in Fe-43.9%Sn-10%Ge ternary alloy, whereas only (Cu) and (Pb) solid solution phases in Cu-35.5%Pb-5%Ge alloy under different undercoolings. In the process of rapid monotectic solidification, α-Fe and (Cu) phases grow in a dendritic mode, and the transition "dendrite→monotectic cell" happens when alloy undercoolings become sufficiently large. The dendrite growth velocities of α-Fe and (Cu) phases are found to increase with undercooling according to an exponential relation.

phase separation, dendrite growth, monotectic alloy, undercooling, macrosegregation

The phase transition pattern and application performance of monotectic alloys have been intensively investigated in the field of material physics in recent years[1−3]. Monotectic solidification involves the nucleation of liquid phase from the second liquid phase and the cooperative growth of solid and liquid phases, providing a complicate and interesting phase transition process, which is significant for the researches on crystal growth dynamics and phase separation mechanism[4,5]. On the other hand, the two solid solutions or intermetallic compounds formed after a monotectic solidification are of different hardnesses, therefore the alloy of this kind will be well used for industrial applications if the second phase distributes uniformly. However, the research on the montectic solidification is focused mainly on the binary monotectic alloys, and the investigation on the

Received March 13, 2007; accepted May 25, 2007
doi: 10.1007/s11433-007-0053-7
†Corresponding author (email: bbwei@nwpu.edu.cn)
Supported by the National Natural Science Foundation of China (Grant Nos. 50121101 and 50395105) and the Doctorate Foundation of Northwestern Polytechnical University of China (Grant No. CX 200419)

crystallization of highly undercooled ternary monotectic alloys is still scarce. The introduction of a third element into a binary alloy influences the nucleation mechanisms and growth kinetics of solidified phases[6−8], and such an effect will become more obvious if the ternary alloy obtains large undercooling. Therefore, the crystallization and rapid growth of ternary monotectic alloys under high undercooling conditions are of importance in both theoretical investigation and practical application. As an efficient method to achieve large undercooling, the glass fluxing method is frequently used for investigating the rapid crystal growth[9−11].

The rapid solidification of undercooled Fe-Sn-Ge and Cu-Pb-Ge alloys was realized by the glass fluxing method. The dendrite growth velocities of the primary α-Fe phase of Fe-Sn-Ge alloy and the primary (Cu) phase of Cu-Pb-Ge alloy were measured under different undercoolings. We discussed the effect of the adding of Ge on the crystal growth kinetics, and revealed the mechanism of the phase separation and the characteristic of monotectic transformation by analyzing solidification microstructures of the ternary monotectic alloys.

1 Experimental procedure

The compositions of Fe-Sn-Ge and Cu-Pb-Ge ternary monotectic alloys were determined by adding 5% and 10% Ge to Fe-Sn and Cu-Pb binary monotectic alloys. Each sample had the mass of 1.0 g, and was prepared from pure Fe (99.99%), Sn (99.99%), Cu (99.99%), Pb (99.99%) and Ge (99.999%). The sample with a suitable mount of dehydrated B_2O_3 was contained in an alumina crucible with the size of ϕ8×10×11 mm, melted by an induction heating equipment and then superheated by 200−400 K for several minutes to ensure homogenization. After that the sample was cooled naturally by switching the power off. The process of heating and cooling was repeated for 3 to 5 times. Its undercoolings were measured by a Yunan-Land NQ08/15C infrared pyrometer which was calibrated with a standard PtRh30-PtRh60 thermocouple, and the crystal growth velocity during rapid solidification was measured by an infrared photodiode device.

After experiments, the solidified samples were sectioned and polished. The solidification microstructures were analyzed by FEI Sirion 200 scanning electron microscope. The phase constitution and thermodynamic properties were determined with a Rigaku D/max2500 X-ray diffractometer and a TA Q1000DSC differential scanning calorimetry analyzer, respectively.

2 Results and discussion

2.1 Phase separation and rapid solidification of the undercooled Fe-Sn-Ge monotectic alloys

(i) Phase constitution analysis. Fe-43.9%Sn-10%Ge monotectic alloy was undercooled to different levels by the glass fluxing method, and the maximum undercooling was 245 K. For lack of the ternary Fe-Sn-Ge phase diagram, differential scanning calorimetry (DSC) was performed to investigate the phase transition process. The sample used for the DSC analysis had a mass of 0.1 g and the heating rate was 10 K/min. The DSC heating curve is presented in Figure 1(a), in which four sharp peaks and a slight step along with the last intensive peak reveal that five phase transitions take place.

XRD analysis was performed to verify the phase constitution of Fe-43.9%Sn-10%Ge alloy. The samples undercooled to different levels are composed of solid solutions α-Fe, (Sn) and intermet-

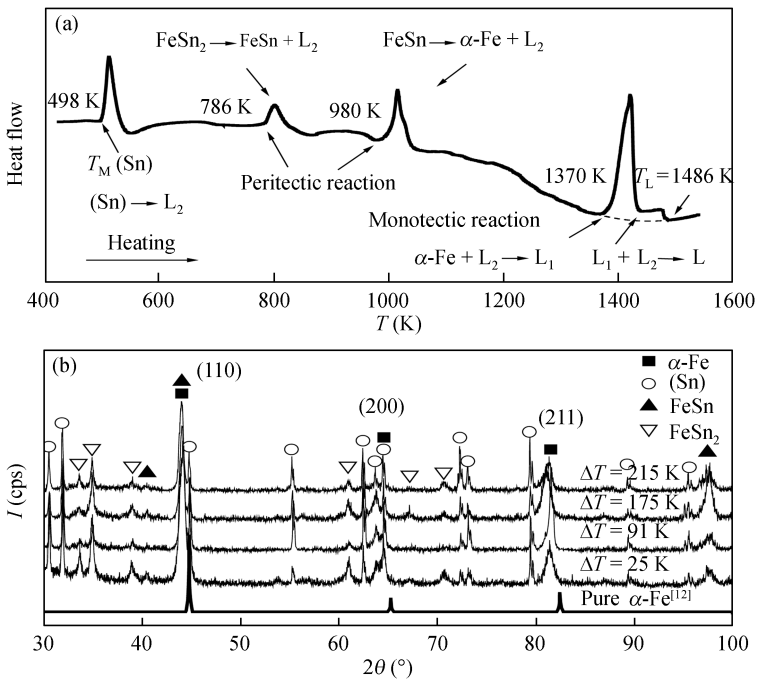

Figure 1 Thermal analysis and X-ray diffraction of Fe-43.9%Sn-10%Ge alloy. (a) DSC thermogram; (b) XRD patterns.

allic compounds FeSn, $FeSn_2$, as shown in Figure 1(b). Based on Fe-Sn binary phase diagram[12,13], the first endothermic peak at 498 K in the DSC curve denotes the melting of (Sn), that is, (Sn) → L_2, L_2 is Sn-rich liquid. This is followed by two endothermic peaks in succession, denoting the decomposion of $FeSn_2$ at 786 K ($FeSn_2 \rightarrow FeSn+L_2$) and FeSn at 980 K ($FeSn \rightarrow \alpha\text{-Fe}+L_2$), respectively. The last peak at 1370 K is correlated to the melting of α-Fe solid phase, that is, $\alpha\text{-Fe} + L_2 \rightarrow L_1$, L_1 is Fe-rich liquid. The heat absorbed during this endothermic peak is nearly equal to the total amount heat absorbed during the other three endothermic peaks. The whole sample was molten totally after the four transitions. As temperature further increases, L_1 and L_2 mix to form homogenous liquid L, that is, $L_1 + L_2 \rightarrow L$. This liquid phase transition needs small heat which leads to only a step occurring in the DSC curve. The liquidus surface temperature is determined to be 1486 K, and the solidus surface temperature is 498 K.

(ii) Characteristics of the rapidly solidified microstructures. The typical solidification microstructures at various undercoolings are presented in Figure 2. The obvious separation of Fe-rich and Sn-rich layer indicates that homogeneous Fe-Sn-Ge melt separates into two liquid phases L_1 and L_2 firstly when the temperature decreases. The obvious difference between the densities of Fe (7.86 g/cm^3) and Sn (7.30 g/cm^3) gives rise to the relative migrations of L_1 and L_2 droplets under gravity condition, as shown in Figure 3(b). High undercooling provides longer time for L_2 droplets to gather and float towards the upper part, resulting in the phase separation going more sufficiently.

When the samples are undercooled to a certain level, monotectic reaction ($L_1 \rightarrow \alpha\text{-Fe} + L_2$) occurs. In the sample with small undercooling, α-Fe phase grows with a relatively slow velocity and forms large coarse dendrites in the lower part. In the upper part, residual L_1 droplets form some Fe-rich monotectic spheres or small dendrites during the monotectic reaction, as shown in Figure 3(c). Figure 2(b) is an enlarged view of the marked part in (a). FeSn and $FeSn_2$ phases as the products of

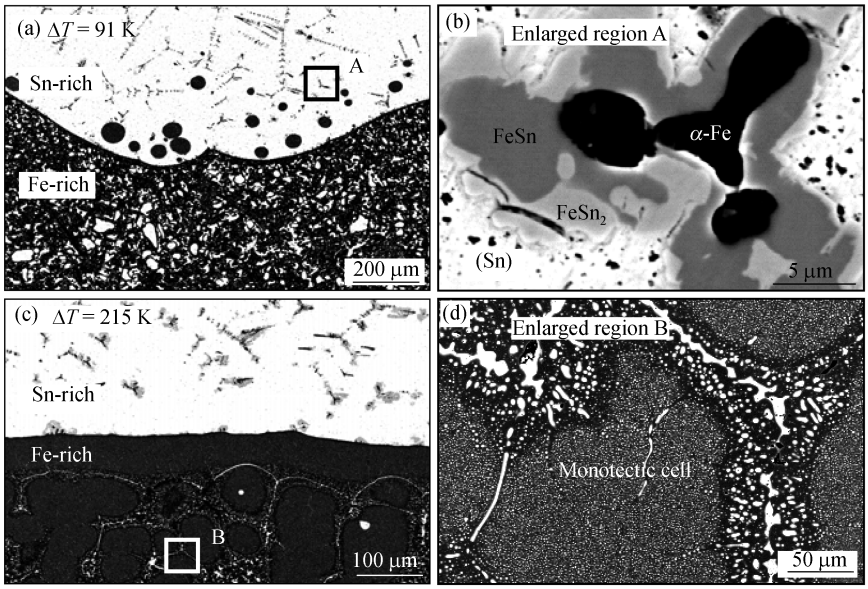

Figure 2 Solidification microstructures of Fe-43.9%Sn-10%Ge alloy at different undercoolings. (a) Microstructures at 91 K undercooling; (b) the enlarged view of region A; (c) microstructures at 215 K undercooling; (d) the enlarged view of region B.

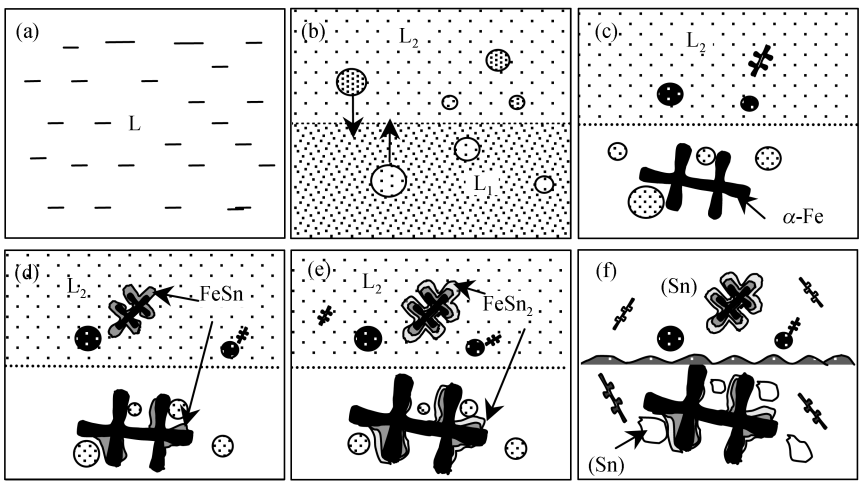

Figure 3 Schematics of solidification process. (a) Homogeneous liquid L; (b) phase separation $L \rightarrow L_1+L_2$; (c) monotectic reaction $L_1 \rightarrow \alpha\text{-Fe} + L_2$; (d) peritectic reaction $\alpha\text{-Fe} + L_2 \rightarrow FeSn$; (e) peritectic reaction $FeSn + L_2 \rightarrow FeSn_2$; (f) final solidification $L_2 \rightarrow$ (Sn).

subsequent peritectic reaction distribute around α-Fe phase, and their forming mechanisms are shown in Figure 3(d) and (e). When the temperature decreases further, L_2 solidifies. The final microstructure of Fe-Sn-Ge alloy with small undercooling is characterized by interdendritic Sn-rich blocks and coarse α-Fe dendrites in the Fe-rich layer, and Fe-rich monotectic spheres and small dendrites in the Sn-rich layer. Comparatively, the alloy with large undercooling solidifies rapidly and monotectic cells form, as shown in Figure 2(c). Figure 2(d) is a local enlarged view of the growth front of a monotectic cell. A large amount of Sn-rich fine particles are distributed homogenously in the matrix of α-Fe phase.

(iii) Growth kinetics of α-Fe phase. According to the DSC curve and XRD analysis, the remarkable recalescence of Fe-43.9%Sn-10%Ge monotectic alloy during the solidification process is associated with the monotectic reaction $L_1 \rightarrow \alpha\text{-Fe}+L_2$. Figure 4 illustrates the relationship between the measured growth velocity of α-Fe dendrite and undercooling. Within the undercooling range 20—245 K, the growth velocity of α-Fe dendrite increases from 1.16 to 224 mm/s. The dendrite growth velocity increases with the increase of undercooling, and their relationship satisfies the following exponential function:

$$V = 4.62\times10^{-3}\left(\mathrm{e}^{1.59\times10^{-2}\Delta T}-1\right). \tag{1}$$

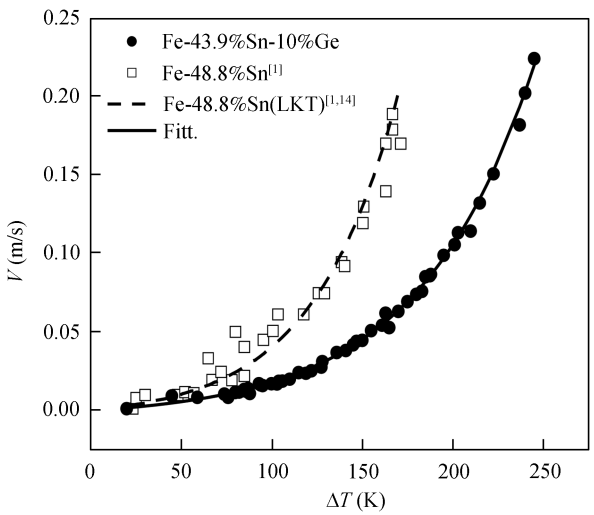

Figure 4 Dendrite growth velocity of α-Fe phase versus undercooling.

The measured and calculated dendrite growth velocities of Fe-48.8%Sn[1,14] are also presented in Figure 4. At the same undercooling level, the growth velocity of α-Fe dendrite in Fe-43.9%Sn-10%Ge ternary alloy is smaller than that in the Fe-48.8%Sn binary alloy, and the deviation is larger at higher undercooling. This is because dendrite growth in the monotectic alloy is always controlled by solute diffusion. The growth of α-Fe dendrite in Fe-Sn-Ge monotectic alloy is controlled by the solute diffusion of both Sn and Ge atoms, and the adding of Ge leads to the remarkable decrease of the dendrite growth velocity.

(iv) Solute trapping effect. The rapid dendrite growth at high undercooling gives rise to the solute trapping, which consequently influences the crystal structure. The XRD pattern of pure α-Fe is also presented in Figure 1(b)[12]. The peaks of α-Fe phase in the Fe-43.9%Sn-10%Ge shift towards a smaller angle compared with that of pure α-Fe phase, which indicates that embedding of Ge and Sn atoms makes the crystal lattice of α-Fe expansion.

The lattice parameter of α-Fe is calculated by measuring the diffraction angles based on Bragg's Law, and the result is presented in Figure 5(a). It is clear that the lattice parameter of α-Fe is larger than that of pure α-Fe, which is 2.867 Å at room temperature[12]. α-Fe lattice parameter increases and then decreases as undercooling increases. For the purpose of interpreting the phenomenon, the solid solubility of α-Fe phase is analyzed. The contents of Ge and Sn in α-Fe phase are shown in Figure 5(b). The solid solubility of Sn shows an increasing tendency whereas Ge increases and then

decreases with the increase of undercooling; the latter is similar to the variation tendency of α-Fe lattice parameter. The lattice parameter of α-Fe solid solutions increases linearly with the Sn content increasing up to 12 wt.%Sn according to Vegard's law[15]. Therefore, the decrease of α-Fe lattice parameter under a substantial undercooling condition is due to the decrease of Ge content. It indicates that both Ge and Sn atoms affect the α-Fe crystal lattice, but Ge atom takes the dominating effect.

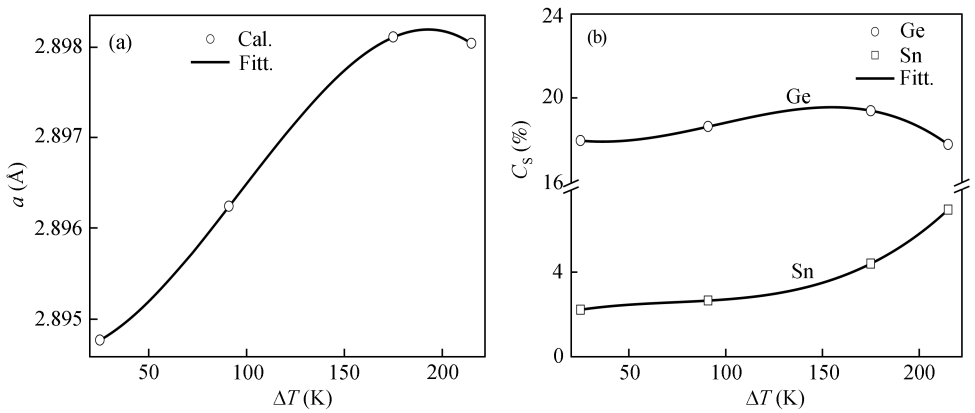

Figure 5 Lattice parameter (a) and solid solubility (b) of α-Fe phase versus undercooling.

2.2 Phase separation and rapid solidification of Cu-35.5%Pb-5%Ge ternary monotectic alloys

(i) Determination of phase constitution. The maximum undercooling of Cu-35.5%Pb-5%Ge ternary monotectic alloy is up to 257 K. For lack of the ternary Cu-Pb-Ge phase diagram, XRD analysis was performed to verify the phase constitution of the samples in order to further investigate the phase transition process and microstructural formation mechanism, and the scan range is 30—90°. The result is presented in Figure 6. It indicates that all the undercooled samples are

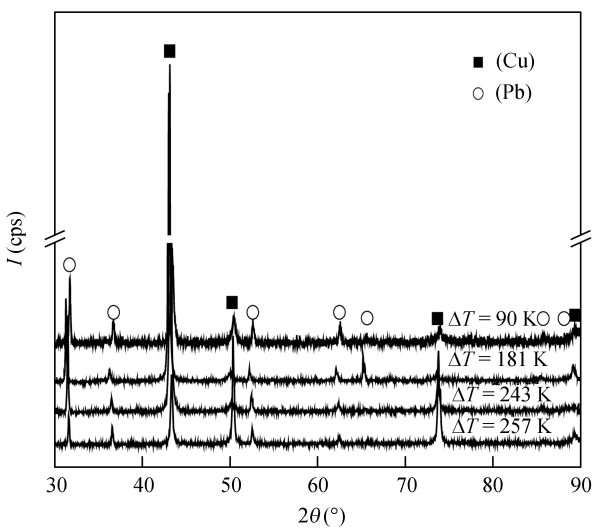

Figure 6 XRD patterns of Cu-35.5%Pb-5%Ge alloy at different undercoolings.

composed of solid solutions (Cu) and (Pb). The phase constitution does not change with undercooling.

(ii) Characteristics of microstructural morphology. In the cooling process, the homogeneous Cu-35.5%Pb-5%Ge melt firstly separates into two liquid phases: $L \rightarrow L_1 + L_2$, in which L_1 is Cu-rich liquid phase and L_2 is Pb-rich liquid phase. On account of the density difference between Pb (11.4 g/cm^3) and Cu (8.96 g/cm^3), the two liquid phases migrate relatively under gravity. Lighter L_1 droplets float up to the sample top whereas heavier droplets sink to the sample accompanied with their cannibal growth. The larger the undercooling is, the longer the phase separation time is and the more thoroughly the liquid phase separation goes. It causes that the two segregation layers become more and more conspicuous. When the samples obtain a certain undercooling, monotectic reaction occurs, $L_1 \rightarrow$ (Cu) $+L_2$. Therefore, the obvious macrosegregation occurs in the microstrutures of undercooled Cu-35.5%Pb-5%Ge monotectic alloy.

Figure 7 is the microstructures of Cu-rich part at different undercoolings. Under small undercooling conditions, (Cu) phase grows in a dendritic manner. With relatively slow growth velocities, very coarse (Cu) dendrites and interdendritic (Pb) blocks form in the upper part. Comparatively, large undercooling leads to a rapid solidification process and thus the uniform monotectic cells form. This microstructural transition is in agreement with that in the Fe-43.9%Sn-10%Ge alloy.

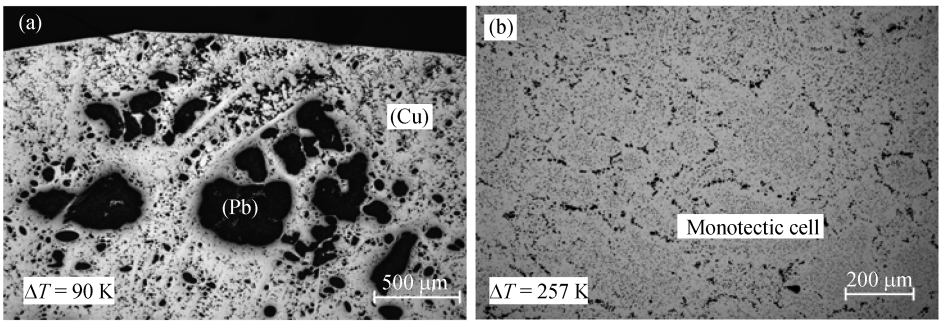

Figure 7 Microstructures of Cu-rich part. (a) Low undercooling; (b) high undercooling.

(iii) Growth kinetics of (Cu) phase. Within the undercooling range of 90—257 K, the dendrite growth velocity of (Cu) phase increases from 11 to 822 mm/s, and the results are shown in Figure 8. With the increase of undercooling, the dendrite growth velocity increases according to the following exponential function:

$$V = 1.25 \times 10^{-6} \left(e^{5.21 \times 10^{-2} \Delta T} - 1 \right). \quad (2)$$

The growth velocity of (Cu) dendrite increases sharply at the undercooling value around 220 K. By analyzing the microstructure of undercooled alloys, we found that the "dendrite—monotectic cell" transition occurs around this undercooling. The cooperative growth of (Cu) and L_2 phase at large undercoolings contributes to the structural morphology transition and the increase of growth velocity.

3 Conclusions

(1) Ternary Fe-43.9%Sn-10%Ge and Cu-35.5%Pb-5%Ge monotectic alloy were undercooled by amounting up to 245 and 257 K, respectively, with the glass fluxing method. XRD analyses reveal

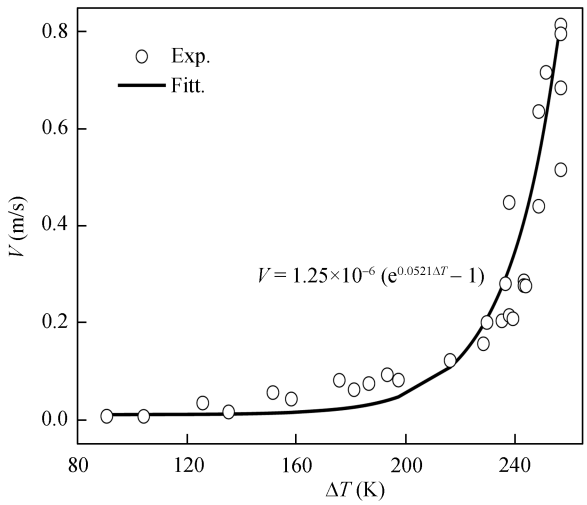

Figure 8 Growth velocity of (Cu) phase versus undercooling of Cu-35.5%Pb-5%Ge alloy.

that the microstructures of undercooled Fe-43.9%Sn-10%Ge alloy consist of four phases including α-Fe, (Sn), FeSn and $FeSn_2$, whereas Cu-35.5%Pb-5%Ge alloy is only composed of (Cu) and (Pb) phases.

(2) Remarkable macrosegregation was observed in both of the ternary Fe-Sn-Ge and Cu-Pb-Ge monotectic alloys and the two segregation layers become more and more conspicuous as undercooling increases. Meanwhile, the microstructures within both separated zones are effectively refined at large undercooling. Once undercooling is sufficiently large, the growth morphologies of α-Fe and (Cu) phases experience a transition from free dendrite to monotectic cell.

(3) In the ternary Fe-43.9%Sn-10%Ge monotectic alloy, the dendrite growth velocity of α-Fe phase varies with undercooling according to the exponential relation $V = 4.62\times10^{-3}(e^{0.0159\Delta T}-1)$. The adding of Ge element apparently reduces the growth velocity of α-Fe dendrites. On the other hand, the lattice parameter of α-Fe phase firstly increases and then decreases with the enhancement of undercooling, which is in agreement with the variation of Ge content inside α-Fe dendrites.

(4) In the ternary Cu-35.5%Pb-5%Ge monotectic alloy, the dendrite growth velocity of (Cu) phase also displays an exponential relation with the variation of undercooling $V = 1.25\times10^{-6}(e^{0.0521\Delta T}-1)$. It is found that the cooperative growth of (Cu) phase and L_2 phase at substantial undercoolings not only results in a structural morphology transition but also enhances the growth velocity of solid phase.

The authors are grateful to Mr. Wan Xiaobo for his help with experiments and Mr. Dai Fuping, Zang Duyang and Wang Haipeng for helpful discussions.

1 Wang N, Wei B. Phase separation and structural evolution of undercooled Fe-Sn monotectic alloy. Mater Sci Eng, 2003, 345: 145－154

2 Tostmann H, Dimasi E, Shpyrko O G, et al. Microscopic structure of the wetting film at the surface of liquid Ga-Bi alloys. Phys Rev Lett, 2000, 84(19): 4385－4388

3 Aoi I, Ishino M, Yoshida M, et al. Influence of growth direction on the microstructure of unidirectionally solidified Cu-Pb monotectic alloy using zone-melt technique. J Cryst Growth, 2001, 222: 806－815

4 Ihle T, Krumbhaar H M. Diffusion-limited fractal growth morphology in thermodynamical two-phase systems. Phys Rev

Lett, 1993, 70: 3083－3086
5 Rosa C D, Park C, Thomas E L, et al. Microdomain patterns from directional eutectic solidification and epitaxy. Nature, 2000, 405: 433－437
6 Wecker J, Helmolt R V, Schultz L. Giant magnetoresistance in melt spun Cu-Co alloys. Appl Phys Lett, 1993, 62: 1985－1987
7 Zhang D L, Cantor B. Effect of Ge on the heterogeneous nucleation of Pb solidification by Al. J Cryst Growth, 1990, 104: 583－592
8 Ratke L, Diefenbach S. Liquid immiscible alloys. Mater Sci Eng, 1995, 15: 263－347
9 Ruan Y, Cao C D, Wei B. Rapid growth of ternary eutectic under high undercooling conditions. Sci China Ser G-Phys Mech Astron, 2004, 47(6): 717－728
10 Kui H W, Greer A L, Turnbull D. Formation of bulk metallic glass by fluxing. Appl Phys Lett, 1984, 45: 615－616
11 Cao C D, Görler G P. Direct measurement of the metastable liquid miscibility gap in Fe-Co-Cu ternary alloy system. Chin Phys Lett, 2005, 22(2): 482－484
12 Giefers H, Nicol M. High pressure X-ray diffraction study of all Fe-Sn intermetallic compounds and one solid solution. J Alloys Comp, 2006, 422: 132－144
13 Hari K K C, Wollants P, Delaey L. Thermodynamic evaluation of Fe-Sn phase diagram. Calphad, 1996, 20(2): 139－149
14 Lipton J, Kurz W, Trivedi R. Effect of growth rate dependent partition coefficient on the dendritic growth in undercooled melts. Acta Metall, 1987, 35(4): 659－970
15 Vegard L. The constitution of mixed crystals and the space occupied by atoms. Z Physik, 1921, 5(17): 17－26